Global Change Biology
celebrating 20 years

Global Change Biology (2015) **21**, 223–235, doi: 10.1111/gcb.12698

The dynamics of architectural complexity on coral reefs under climate change

YVES-MARIE BOZEC[1,2], LORENZO ALVAREZ-FILIP[3] and PETER J. MUMBY[1,2]

[1]*Marine Spatial Ecology Lab, ARC Centre of Excellence for Coral Reef Studies, School of Biological Sciences, University of Queensland, St. Lucia, Qld 4072, Australia,* [2]*College of Life Sciences, University of Exeter, Exeter EX4 4PS, UK,* [3]*Unidad Académica de Sistemas Arrecifales, Instituto de Ciencias del Mar y Limnología, Universidad Nacional Autónoma de México, Puerto Morelos, Quintana Roo 77580, México*

Abstract

One striking feature of coral reef ecosystems is the complex benthic architecture which supports diverse and abundant fauna, particularly of reef fish. Reef-building corals are in decline worldwide, with a corresponding loss of live coral cover resulting in a loss of architectural complexity. Understanding the dynamics of the reef architecture is therefore important to envision the ability of corals to maintain functional habitats in an era of climate change. Here, we develop a mechanistic model of reef topographical complexity for contemporary Caribbean reefs. The model describes the dynamics of corals and other benthic taxa under climate-driven disturbances (hurricanes and coral bleaching). Corals have a simplified shape with explicit diameter and height, allowing species-specific calculation of their colony surface and volume. Growth and the mechanical (hurricanes) and biological erosion (parrotfish) of carbonate skeletons are important in driving the pace of extension/reduction in the upper reef surface, the net outcome being quantified by a simple surface roughness index (reef rugosity). The model accurately simulated the decadal changes of coral cover observed in Cozumel (Mexico) between 1984 and 2008, and provided a realistic hindcast of coral colony-scale (1–10 m) changing rugosity over the same period. We then projected future changes of Caribbean reef rugosity in response to global warming. Under severe and frequent thermal stress, the model predicted a dramatic loss of rugosity over the next two or three decades. Critically, reefs with managed parrotfish populations were able to delay the general loss of architectural complexity, as the benefits of grazing in maintaining living coral outweighed the bioerosion of dead coral skeletons. Overall, this model provides the first explicit projections of reef rugosity in a warming climate, and highlights the need of combining local (protecting and restoring high grazing) to global (mitigation of greenhouse gas emissions) interventions for the persistence of functional reef habitats.

Keywords: bleaching and hurricanes, habitat loss, hindcast and forecast simulation, mechanical stress, parrotfish erosion, structural complexity

Received 5 May 2014; revised version received 17 July 2014 and accepted 25 July 2014

Introduction

One striking feature of coral reef ecosystems is the development of three-dimensional (3-D) limestone structures that enhance living and refuge space for a multitude of organisms. Complex reef architectures typically support diverse and abundant biological communities (reviewed by Graham & Nash, 2013) by facilitating the survival of organisms through the mediation of critical ecological processes, including recruitment, predation and competition (e.g. Jones, 1991; Hixon & Beets, 1993; Syms & Jones, 2000). While the reef architecture is an important driver of the reef community structure, complex architectures are often observed on reefs with an extensive cover of live corals (Alvarez-Filip *et al.*, 2011; Graham & Nash, 2013), especially when complex (e.g. branching) or large massive coral life-forms dominate (Rogers *et al.*, 1982; Steneck, 1994; Alvarez-Filip *et al.*, 2011). Yet reef-building corals are in decline worldwide (Gardner *et al.*, 2003; Bruno & Selig, 2007; De'ath *et al.*, 2009) and a general loss of architectural complexity has been reported in the Caribbean in the past four decades (Alvarez-Filip *et al.*, 2009a).

Central to the creation of the reef relief is the growth and calcification of hard corals that constitute the structural units of the superficial reef framework (e.g. Hubbard *et al.*, 1998; Perry *et al.*, 2008), even though the accretion of reefs over geological time scales incorporates many other factors (Shinn *et al.*, 1982; Perry *et al.*, 2008). While coral skeletons extend the reef surface through carbonate accretion and cementation, a number of biological and physical agents lead to the erosion of the upper carbonate framework (Hutchings,

Correspondence: Yves-Marie Bozec, Marine Spatial Ecology Lab, School of Biological Sciences, University of Queensland, St. Lucia, Qld 4072, Australia, tel. +61 7 33 651 671, fax +61 7 33 651 655, e-mail: y.bozec@uq.edu.au

1986; Glynn, 1997; Tribollet & Golubic, 2011). The balance between these constructive (accretion) and destructive (erosion) processes determines the ability of the reef surface to grow through net carbonate accretion (Stearn *et al.*, 1977; Perry *et al.*, 2008, 2012). Yet, recent carbonate budgets of Caribbean reefs have revealed significant reductions in their ability to sustain a net reef accretion (Kennedy *et al.*, 2013; Perry *et al.*, 2013). Considering the importance of corals in the production of reef carbonate, and the predicted impacts of climate change on coral growth and calcification (Hoegh-Guldberg *et al.*, 2007; Anthony *et al.*, 2011; Frieler *et al.*, 2012), there is a growing concern over the ability of coral reefs to maintain functional habitat structures in the future (Hoegh-Guldberg *et al.*, 2007; Kennedy *et al.*, 2013). A failure of reefs to maintain a positive carbonate budget will likely lead to a decline in many ecosystem services including biodiversity, fisheries productivity and recreational value (Done *et al.*, 1996).

While a negative carbonate budget implies a net loss of reef framework, it gives little indication of the consequences for the *quality* of the reef habitat structure (i.e. the complexity of its superficial architecture), which has a functional impact on reef-associated organisms. The complexity of the reef habitat is typically captured by its topography (McCormick, 1994; Jones & Syms, 1998), yet little is known about the rate of loss of topographical complexity associated with a negative reef carbonate budget. Habitat is a multi-scale concept but community-based studies have mostly investigated topographical patterns at the scale of metres (from 1 to 10s of metres). At this scale, processes shaping reef topography are those affecting the growth of living and erosion of dead coral skeletons, and such processes operate at relatively short (as opposed to geological times) temporal scales (e.g. <100 years, Perry *et al.*, 2008). The response of coral-scale (1–10 m) topographical complexity to erosion likely depends (1) on species-specific rates of coral mortality in response to disturbances, such as bleaching and hurricanes, and (2) the loss of complexity caused by the erosion of structurally different carbonate skeletons. Therefore, quantifying the contribution of each coral species to the reef surface topography, through the complexity of their skeleton during both the accreting (live) and eroding (dead) phases is key for estimating the degradation of colony-scale habitat complexity on net eroding reefs. Predicting the dynamics of reef structural complexity is of particular importance to envision the future functioning of reefs and their ability to support ecosystem services (Pratchett *et al.*, 2014; Rogers *et al.*, 2014).

Here, we develop and test a mechanistic model of reef topographical complexity for contemporary Caribbean reefs. The model describes the dynamics of corals and other benthic taxa under the control of multiple disturbances (hurricanes and coral bleaching), and is calibrated using observed changes on the reef benthic structure in Cozumel (Mexico) on decadal time scales. Providing corals have a simplified shape with explicit diameter and height, the model calculates carbonate accretion and erosion at the scale of a coral colony, simulating changes in coral volume and surface and their impact on the reef topographical complexity. Model simulations are used to investigate possible scenarios of change in reef topographical complexity in response to global warming under different hurricane and local management (i.e. parrotfish protection) regimes.

Materials and methods

Model overview

A mechanistic model of reef topographical complexity was developed by extending a two-dimensional (2-D) model of coral populations (Mumby, 2006; Mumby *et al.*, 2006, 2007; Edwards *et al.*, 2011) to quantify the contribution of the 3-D structure of coral colonies to the extension of the reef surface. The 2-D model is designed to simulate coral-algae dynamics in a regular square lattice of 400 cells, each approximating 1 m^2 of a typical mid-depth (5–15 m) Caribbean forereef. Individual cells can be occupied by multiple coral colonies of different species and patches of cropped algae (a mixture of coralline algae and short turf) or macroalgae (*Dictyota pulchella*, *Lobophora variegata*). Each coral colony is defined by its cross-sectional (circular) basal area on the square lattice. Starting from a given size structure and absolute cover area, coral colony sizes (in cm^2) are updated every 6 month following systematic and probabilistic rules which reflect processes of coral population dynamics (recruitment, colony growth, predation and natural mortality), macroalgal populations (growth and grazing from herbivores) and coral-algae interactions (competition for space). As a result, coral populations grow if the grazing pressure is high enough to maintain macroalgae in a cropped state (short turf) so that space is freed for coral growth and recruitment (Mumby, 2006). However, coral populations in the model are subject to bleaching and hurricanes that can occur either randomly or following a predefined schedule, both disturbance regimes being able to impair the persistence of a coral-dominated state (Edwards *et al.*, 2011; Mumby *et al.*, 2013). A full description of model components, rules, parameters and assumptions is provided in Appendix S1.

Model implementation of topographical complexity

Reef topographical complexity is commonly assessed in the field using the chain-and-tape method (Risk, 1972) where a fine chain is draped over the reef bottom surface along short (from 3 to 20 m, Knudby & LeDrew, 2007; Alvarez-Filip *et al.*, 2009a) transect lines. Dividing the chain length by the

horizontal distance it covers produces an index of surface roughness or rugosity (Luckhurst & Luckhurst, 1978; McCormick, 1994). The rugosity index approximates how much the 3-D reef surface departs from its 2-D projection on an horizontal plane: the higher the ratio, the greater the deformation of the reef bottom. As a result, high rugosity values (i.e. >2.5) are typically found in rich coral areas dominated by complex life-forms, such as the large branching acroporids, whereas low rugosity values (i.e. <1.5) are characteristics of coral-depauperate reefs or reefs dominated by diminutive coral forms (Rogers *et al*., 1982; Steneck, 1994; Alvarez-Filip *et al*., 2011).

Assuming that the extension of the reef surface is primarily driven by coral growth and calcification, corals can be considered as building blocks that successively generate the formation of 3-D carbonate structures. Here, corals are stylised by circular paraboloid volumes, i.e. solids of revolution obtained by rotating a parabola around their axis of symmetry (Fig. 1a). Like the 2-D grid model, coral growth is modelled by the cross-sectional basal area of coral colonies (i.e. their planimetric projection on the grid lattice) which grows laterally at a rate that is species-specific (listed in Appendix S1, Table S1). For every radial increment, colony height is calculated from empirical relationships derived from field data (see parametrization below), so that coral colonies can grow vertically over time (Fig. 1b). Designing a regular solid shape for corals facilitates the calculation of colony surface area and volume through the use of standard geometric formula, based on diameter and height (see Appendix S1, Eqns S1 and S2). As a result, the volume and actual surface area of living colonies increase over time as the colonies grow in three dimensions.

When an entire colony dies, its skeletal structure becomes a new substrate covered by short algal turf, thus extending the reef framework surface that can be colonised by corals and macroalgae. Here, dead corals are a new class of object enabling the representation of the upper carbonate framework of the reef. Like living corals, the spatial arrangement of dead corals is not explicit, but skeletal material accumulates within the cell (Fig. 1c). Dead skeletons are subject to external erosion driven by excavating parrotfish and it is assumed that urchin abundance is functionally absent, including *Echinometra*. The total volume of carbonate that is eroded at every time step is fixed for the whole reef grid. Colony volume after external erosion is used to recalculate the height of dead skeletons (Eqn S2) based on the simplifying assumption that basal colony diameter is kept constant during grazing erosion (Fig. 1b). As such, external bioerosion is directed towards the top of coral colonies in conformity with the observation that excavating parrotfish preferentially erode convex surfaces (Bellwood & Choat, 1990; Bruggemann *et al*., 1996; Ong & Holland, 2010). As a result, grazing erosion flattens individual dead skeletons, thus reducing reef substrate area at every time increment. Erosion by infaunal bioeroders (e.g. sponges, bivalves, worms and cyanobacteria, Tribollet & Golubic, 2011) is assumed not to affect the shape of coral skeletons; rather, internal erosion increases skeletal porosity, and, consequently, susceptibility to storm-induced breakage (see details below).

The model tracks the individual production/erosion of carbonate skeletons which drives the pace of extension/reduction

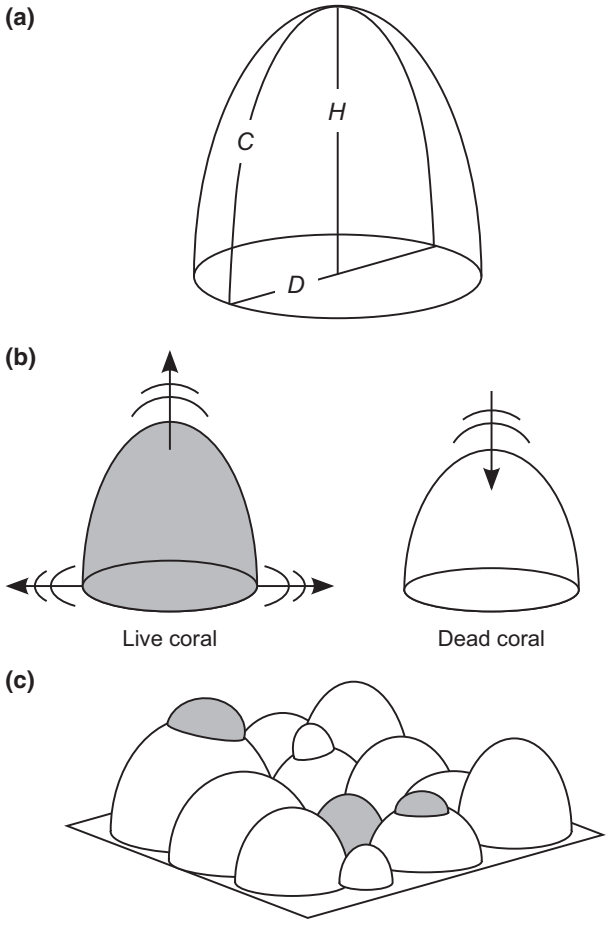

Fig. 1 Model assumptions for the representation of the 3-D structure of the reef bottom: (a) geometry of a circular paraboloid as a proxy of coral colony shape (*D*: diameter, *H*: height, *C*: contour); (b) morphological changes of living (left panel) and dead (right panel) coral colonies over time: coral growth extends colony diameter and height, whereas external erosion decreases colony height of dead corals; (c) schematic illustration of the reef bottom built from the accumulation of dead (white paraboloids) and living (grey paraboloids) corals within a model grid cell. The exact position of coral colonies within a cell is actually unknown.

of the reef surface. Surface and planimetric areas of dead colonies are combined (Eqn S3) to estimate the surface area of the dead carbonate framework (hereafter referred to as "reef substrate") in every grid-cell. As a result, the reef substrate area is changing over time depending on the extent of coral mortality and erosion. One implication is that transient changes in reef substrate area dynamically influence spatial ecological processes such as grazing intensity and competition between corals and algae (see details in Appendix S1).

Both dead and living coral colonies contribute to the topographical complexity of a reef. At every time step, the actual surface area of the reef bottom is estimated by combining the surface and planimetric areas of living corals with the reef

substrate area (Eqn S5). A surface-to-area ratio is then calculated (Eqn S6) for the whole reef grid by dividing the surface area of the reef bottom by its planimetric projection (i.e. the horizontal area of the reef grid). The higher the ratio, the greater the deformation of the reef bottom thus providing an index of surface roughness for the modelled reef. Here, surface roughness is not a strict equivalent to the rugosity index assessed in the field, the latter capturing only the deformation of the reef bottom based on its vertical (2-D) profile. However, we assume the two indices of topographical complexity are proportional, in a similar manner to the surface-to-area and contour-to-linear ratios relationships at colony scales. An empirical relationship between reef rugosity and surface roughness was derived from the systematic analysis of 3-D and 2-D morphometrical ratios of paraboloids of increasing diameter and height (see details in Appendix S1). This relationship allowed us to convert reef surface roughness into a field-relevant rugosity index at any time step of the model.

Parametrization of colony shape: observed coral morphology

Coral morphometric data collected on reefs in south-western Cozumel (Mexican Caribbean) in April 2009 were used to derive empirical relationships between colony diameter and colony height and to test the assumption that the shape of massive and submassive coral colonies can be approximated by a circular paraboloid. Coral colonies were randomly sampled at middepth (7–14 m) in four sites and the following measurements were taken: (1) maximum horizontal extension (~colony diameter); (2) maximal vertical extension (~colony height) and (3) the contoured length measured along the maximum horizontal extension (~colony contour). As for the simulation model, we assume that the sampled colonies can be represented by regular disks on the horizontal plane, with a diameter equal to the maximum horizontal extension measured.

Colony height (H) was modelled using linear regression with colony diameter (D) as predictor for the seven most represented species: *Agaricia agaricites* (n = 73), *Porites astreoides* (n = 51), *Siderastrea siderea* (n = 42), *Montastraea cavernosa* (n = 35), *Orbicella faveolata* (n = 24), *Orbicella annularis* (n = 22) and *Porites porites* (n = 19). For every species, H and D were square root transformed to meet the assumption of normality, and linear models were designed with forced zero intercepts. This produced seven empirical relationships that were used in the simulation model to update the height of living corals for every radial increment specified by the species growth rates.

To validate our assumption of paraboloid coral colonies, we calculated the contour (C) of every sampled coral colony using its observed D and predicted H. The contoured length of a circular paraboloid corresponds to the length of the parabolic arc and is given by (Stine & Geyer, 2001):

$$\hat{C} = \frac{D^2}{8\hat{H}} \ln\left[\frac{4\hat{H}}{D} + \sqrt{\left(\frac{4\hat{H}}{D}\right)^2 + 1}\right] + \frac{D}{2}\sqrt{\left(\frac{4\hat{H}}{D}\right)^2 + 1} \quad (1)$$

For each coral species, predicted and observed C were compared using the Spearman's rank correlation coefficient, high correlations indicating that the paraboloid shape is an acceptable proxy of actual coral colony shape.

Model calibration: Cozumel reef data (1984–2008)

The model was calibrated using historical benthic surveys of the leeward reefs in south-western Cozumel, compiled from literature and published reports (Appendix S2, Table S3). We selected data on benthic cover reported on middepth (5–20 m) inner reefs and shelf-edge reefs, where sand cover did not exceed 25%. The unit of observation is a reef site according to the definition of a reef in the simulation model (20 × 20 m). When available, within-site samples (i.e. transects) were averaged to produce a site-level estimate of benthic cover, and every record was assigned to the appropriate season as defined in the simulation model (*summer*: July to December; *winter*: January to June). The resulting data series runs for twenty-four years (August 1984–May 2008). Site description and selection are detailed in Appendix S2.

Coral cover. Model initialization was set up with a 31% coral cover, which corresponds to the average reported during the period 1984–88 (n = 25 reefs) before hurricane Gilbert hit the coast of Cozumel in September 1988. Based on the description of coral composition (Appendix S2, Table S4), initial coral cover was distributed among the same seven coral species used in the parametrization phase (% relative cover): *A. agaricites* (53%), *P. porites* (24%), *O. annularis* (7%), *O. faveolata* (7%), *M. cavernosa* (4%), *P. astreoides* (3%), *S. siderea* (2%). In the model, *A. agaricites* included the polymorph *A. tenuifolia* which was the most common coral on the tops of the shelf-edge reefs in the mid 1980s. *P. porites* includes *P. furcata* which has a similar digitate morphology. As a result, those seven species represented 90% and 95% of the total coral cover surveyed in 1984–1988 and 2005, respectively. For each model initialization, coral species covers were randomized following a normal distribution (see details in Appendix S1) to reproduce the variability (22–49%) observed on total coral cover in 1984–1988. Parametrization of other benthic covers (i.e. macroalgae, sponges and ungrazable cover) is detailed in Appendix S2.

Topographical complexity. Unfortunately, the only available data for topographical complexity were collected in 2007–2008 (Alvarez-Filip *et al.*, 2011). At this time, reef rugosity was 1.5 on average and strongly correlated with total coral cover (Appendix S2). Initial reef rugosity was therefore derived from the initial coral cover (31%) using Alvarez-Filip *et al.* (2011)'s empirical relationship between reef rugosity and total coral cover, assuming the two metrics exhibited the same relationship at the start of the time-series. From this relationship we extrapolated an average rugosity value of 1.9 which was further randomised following a normal distribution (see details in Appendix S1).

Parrotfish grazing and bioerosion. Reefs in south-western Cozumel have been protected since 1980 (Fenner, 1988) and

currently support high parrotfish abundances and biomasses (LAF and PJM, pers. obs.), especially *Sparisoma viride* and *Scarus vetula* which are very efficient grazers. Therefore, maximum grazing impact (Appendix S1) was set to 40% of the actual surface of the reef substrate grazed, which is representative of a reef with unfished parrotfish populations (Mumby, 2006).

Parrotfish bioerosion in the Caribbean is mainly due to *S. viride* and large individuals of *S. vetula* (Frydl & Stearn, 1978; Bruggemann *et al*., 1996). In the absence of detailed data on the size composition of parrotfish assemblages in Cozumel, we simulated different bioerosion rates falling into the range of published grazing erosion values (0.01–7.62 kg $CaCO_3$ m^{-2} yr^{-1}, (Bruggemann *et al*., 1996; Mallela & Perry, 2007; Perry *et al*., 2012). Each tested value of parrotfish erosion was scaled to the dimension of the model grid (20 × 20 m), then converted into a total volume (cm^3) of carbonate to be removed from the grid every 6 month, assuming a standard density of 1.7 g cm^{-3} for carbonate skeletons (Perry *et al*., 2012). Parrotfish bioerosion was concomitant with grazing, so that the eroded surface of dead skeletons equalled the area grazed, and the cumulated volume eroded in every cell matched the volume specified at the reef scale (see details in Appendix S1).

External disturbances: hurricanes and bleaching. Modelled reefs were subject to the actual regime of major category hurricanes (i.e. category 3 and higher on the Saffir-Simpson scale) that occurred between 1984 and 2008 in Cozumel: hurricanes Gilbert in 1988 (category 5), Roxanne in 1995 (category 3), and Emily (category 4) and Wilma (category 4) in 2005. We allowed for two hurricanes during summer 2005 to represent the cumulative damages caused by Emily and Wilma. Because patterns of reef damages caused by hurricanes are typically patchy (e.g. Woodley *et al*., 1981; Rogers *et al*., 1982), the occurrence of a scheduled hurricane was further randomized for each replicate simulation. For a simulated reef, the probability to be impacted by a scheduled hurricane (Appendix S1) was derived from the observed proportion of Cozumel reef sites that were significantly damaged by hurricanes Gilbert (Fenner, 1991) and Emily-Wilma (Alvarez-Filip *et al*., 2009b).

When occurring, hurricanes cause whole-colony (dislodgement) and partial (fragmentation) coral mortalities due to mechanical stress. Similar to (Edwards *et al*., 2011), colony breakage is a function of hurricane category and colony size, but here rates of breakage were further adapted to each coral species based on species-specific losses reported in Cozumel (Appendix S1). While the fragility of recently dead skeleton is likely similar to that of living colonies, susceptibility to breakage after death may either increase with internal bioerosion (i.e. macro- and microboring) or decrease with cementation by binding agents (i.e. calcareous encrusters). Because the extent and timing of these processes are unknown, we simply assumed that the probabilities of breakage of dead skeletons were proportional to those of their living counterparts, with a magnitude factor to be determined by fitting the model to Cozumel observations. This was implemented using a global multiplier of coral mortalities (hereafter referred to as breakage susceptibility relative to live corals), identical for all species of dead corals and varying from 0 to 2. In this way, the net effects of cementation and internal erosion are encapsulated implicitly in the probability of breakage without requiring a complex and highly uncertain parametrization. Dislodged colonies and fragments (dead and alive) were removed from the model grid assuming transport and dispersion off the reef.

We also allowed for bleaching events to occur based on Cozumel waters thermal climatology for the period 1984–2008. Weekly based sea surface temperatures (SST) recorded by NOAA at Cozumel were converted into Degree Heating Weeks (DHWs) similar to (Edwards *et al*., 2011). DHWs allowed the calculation of coral mortality (see details in Appendix S1) following the empirical data of Eakin *et al*. (2010). Bleaching did not occur if a hurricane had occurred that year.

Model performance. A total of 100 model simulations were run over 48 seasonal time steps (from summer 1984 to winter 2008) to compare the simulated coral cover and reef rugosity with observations from Cozumel. Model performance was assessed through its ability to meet three objectives: (1) reproduce the observed average and variability in total coral cover over time; (2) reproduce the relative cover of the dominant species (*A. agaricites*, *P. porites* and *O. annularis*) as observed before and after the 2005 hurricane season (Alvarez-Filip *et al*., 2009b); (3) reproduce the relationship between total coral cover and rugosity as observed in 2007–2008 (Alvarez-Filip *et al*., 2011). Considering the high uncertainty associated with parrotfish bioerosion and susceptibility of dead skeletons to breakage caused by hurricanes, different values of these two parameters were tested until the agreement between simulations and observations, based on visual judgement, were reasonably good. No statistical procedure was applied for optimising simulations, considering that a better fit to observations will not increase confidence in the adjusted parameter values of mechanical and biological erosion. However, we report the relative influence of the two erosion rates on model outputs (final coral cover and rugosity) for a critical evaluation of erosion and its relative importance on model performance, given the uncertainty of observations.

Model application: future scenarios of topographical complexity

The model was finally used to explore long-term (40 years) scenarios of changing rugosity for a Caribbean reef submitted to future thermal stress and different regimes of hurricanes. Bleaching events were scheduled according to future SST as predicted by the UK Hadley Centre Global Environmental Model HadGEM1 (Johns *et al*., 2006) following the Representative Concentration Pathway (RCP) 8.5 trajectory for greenhouse gases (GHG), a warming scenario which considers high, "business as usual" GHG emissions (Riahi *et al*., 2011). The simulated scenarios used the Caribbean basin mean SST (Edwards *et al*., 2011) calculated monthly from 2010 to 2050 to calculate degree heating weeks which determine the probability of coral bleaching (Appendix S1). We therefore assumed that the response of corals to bleaching is dominated by the

intensity of acute thermal stress and not modified by acclimation/adaptation. Hurricanes occurred randomly with a low (0.05) and high (0.2) probability to contrast the effects of different hurricane regimes (one every 20 years vs. one every 5 years on average) on reef rugosity. When a hurricane occurs, its strength (Saffir-Simpson categories 1–5) is determined randomly with an equal chance for each category.

Model simulations were used to estimate the average time for a present-day Caribbean reef to lose its topographical complexity. For the two scenarios of hurricane frequency, the model was initialized with increasing total coral cover (from 2 to 25% by increments of 1%) and rugosity (from 1.3 to 2 by increments of 0.05) to explore a wide range of reef architectures. Total coral cover at initial step was distributed across the seven coral species with the same relative covers used to reconstruct Cozumel reef trajectories. For each coral/rugosity combination we calculated the average time step at which reef rugosity falls below 1.2 based on a minimum of 40 replicate simulations. A threshold of 1.2 was chosen because it represents the Caribbean average at the end of a recent meta-analysis of reef rugosity on Caribbean reefs (Alvarez-Filip *et al.*, 2009a). The two hurricane scenarios were run for a high (40%) and medium (20%) grazing impact for evaluating the effects of managed (fully protected) vs. unmanaged (fished) parrotfish populations on the future predictions of reef rugosity. Parrotfish bioerosion was reduced proportionally to grazing impact to balance the indirect, positive effects of parrotfish grazing on the persistence of corals with the direct, negative effects of parrotfish erosion on topographical complexity.

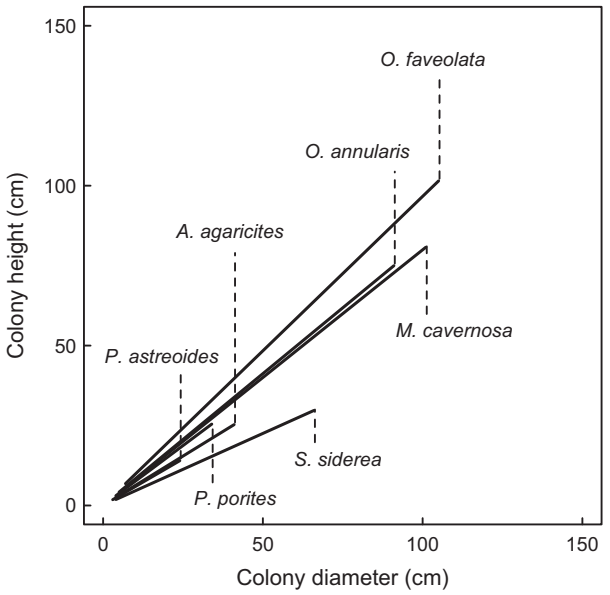

Fig. 2 Linear regressions of colony height as a function of colony diameter for the seven coral species based on Cozumel *in situ* measurements (see Appendix S3, Fig. S4 for detailed relationships and related statistics).

Results

Coral colony morphometrics

The analysis of *in situ* morphometric measurements showed that colony height is linearly related to colony

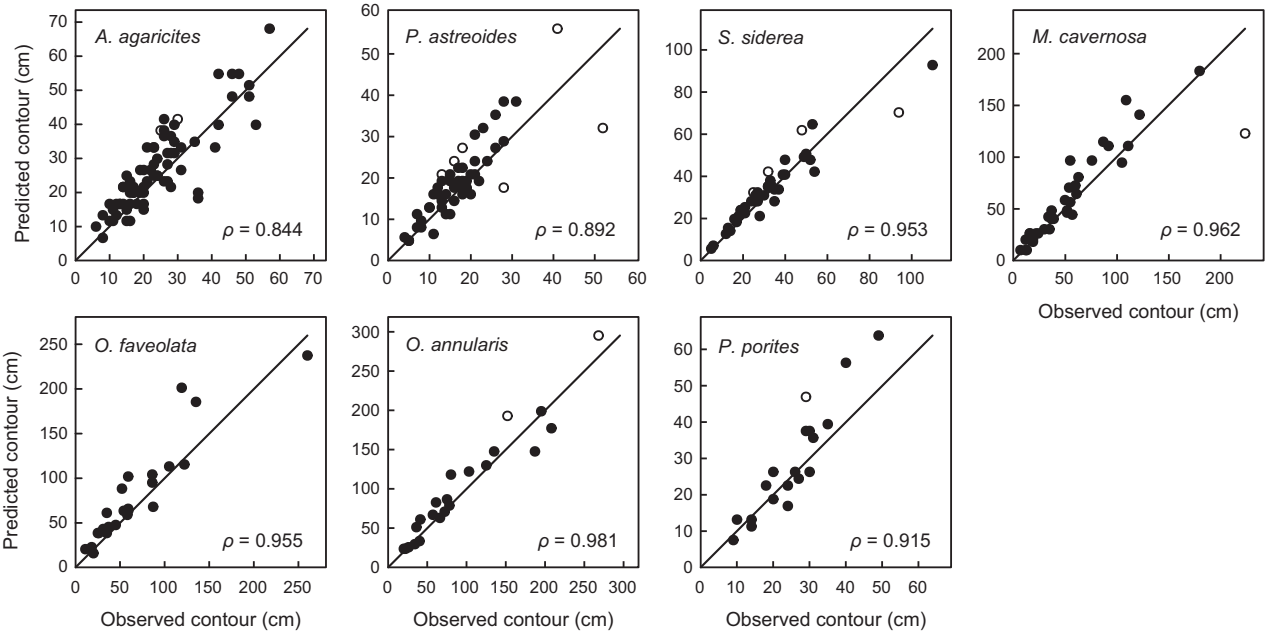

Fig. 3 Relationship between predicted and observed colony contours (full circles) for the seven coral species. Empty circles indicate outliers (details in Appendix S3, Fig. S4). The Spearman's rank correlation coefficient (ρ) is significantly non null at $P < 0.001$ for every coral species. Solid lines represent a 1 : 1 relationship.

diameter for the seven coral species (Fig. 2; Appendix S3, Fig. S4). Colony height increased more quickly with diameter (i.e. steeper slope) for the three mound-like species, *M. cavernosa*, *O. faveolata* and *O. annularis*. These species also included coral colonies with the largest diameter (up to 100 cm). Species departing from a mound-like shape, such as *A. agaricites* (weedy/encrusting colonies) and *P. astreoides* (boulder/encrusting colonies) exhibited the weakest, although significant, relationship.

To test for the ability of paraboloids to approximate coral colony shapes, we calculated the expected contoured lengths of *in situ* coral colonies under a paraboloid model (Eqn 1), based on their observed diameter and predicted height (i.e. as estimated by the empirical relationships). Expected colony contours were highly correlated with the contours measured *in situ* for all coral species (Fig. 3), with highest correlations obtained for boulder and mound-like coral shapes (*S. siderea*, *M. cavernosa*, *O. faveolata* and *O. annularis*). As a consequence, the contour indices (i.e. the ratio of the contoured length to the largest diameter) calculated from *in situ* colonies were very similar to those expected under a paraboloid model (Appendix S3, Fig. S5 and Table S5).

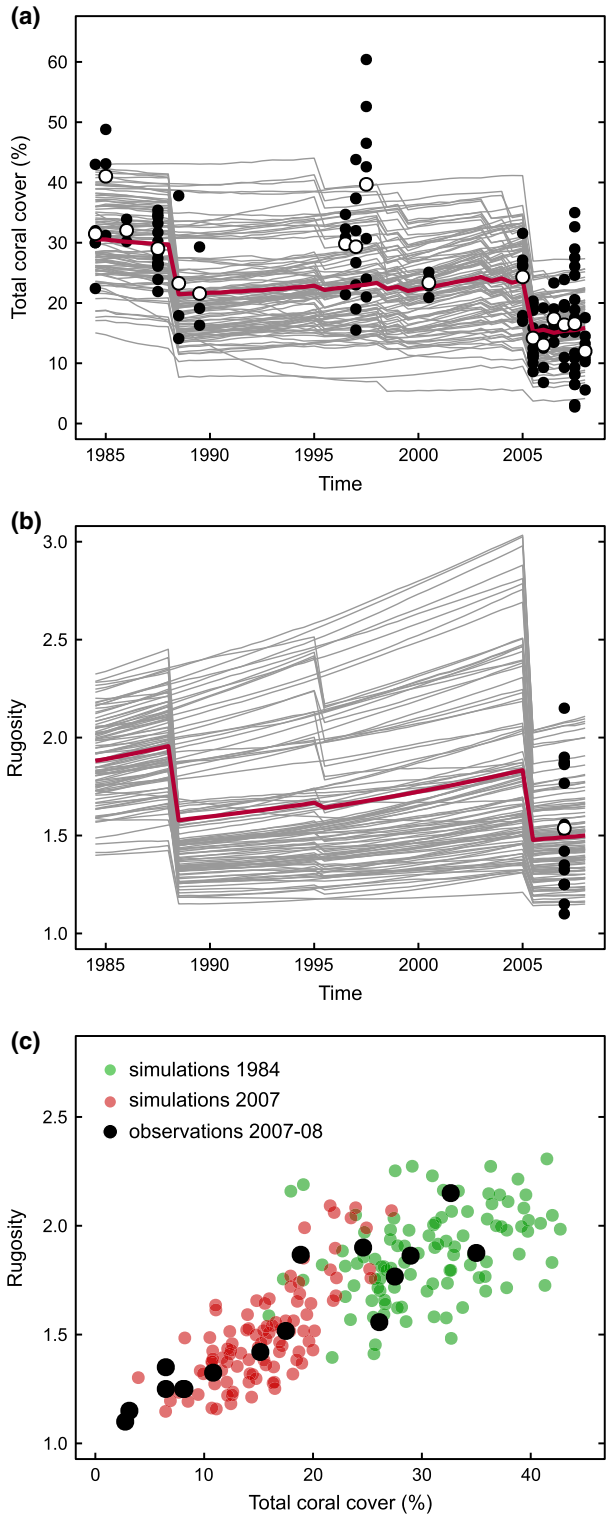

Historical trajectories of reefs in Cozumel

Model simulations between 1984 and 2008 closely matched the observations of total coral cover reported in Cozumel (Fig. 4a), except for the 1996–1997 observations where average coral cover has been estimated at around 30–40% while simulations predicted a 25% average at this time. In 25 years, coral populations have declined from a cover of ~31% to ~16%. Simulations and observations per coral species (Fig. 5) suggested that this decline was mostly due to losses in the cover of *A. agaricites* (from 18% to 5%) and *P. porites* (from 8% to 0.5%). Model and data indicated that coral losses were due to mortalities induced by hurricanes (−10% after hurricane Gilbert in 1988, −11% after hurricanes Emily-Wilma in 2005). Just before the 2005 hurricane season, *P. porites* populations had recovered the cover exhibited before hurricane Gilbert (~8%). In contrast, the *A. agaricites* population in 2005 failed to recover its

Fig. 4 Reconstructed trajectories of total coral cover (a) and reef rugosity (b) between 1984 and 2008 on south-western Cozumel reefs, and relationship (c) between simulated reef rugosity and total coral cover at the start (green dots) and at the end (red dots) of the modelled period. Grey lines and red lines in (a) and (b) represent, respectively, the individual and average reef trajectories of coral cover and rugosity predicted by the model. Black dots represent the observed site averages and open dots the global averages for a given season. Regression equations in (c): 2007–2008 observations, $y = 1.072 + 0.027\,x$ ($R^2 = 0.85$, $P < 0.001$, $N = 16$); 2007 predictions, $y = 0.914 + 0.037\,x$ ($R^2 = 0.37$, $P < 0.001$, $N = 100$).

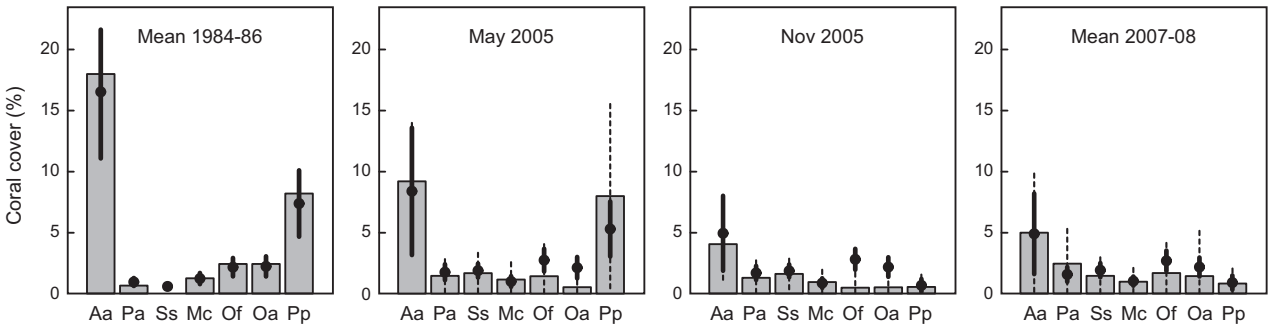

Fig. 5 Comparison of the species (average) absolute per cent cover between *in situ* observations (grey bars) and model predictions (black dots) at different time steps between 1984 and 2008. Error bars indicate standard deviations around the observed (dotted line) and simulated (thick line) averages. Aa = *A. agaricites*, Pa = *P. astreoides*, Ss = *S. siderea*, Mc = *M. cavernosa*, Of = *O. faveolata*, Oa = *O. annularis*, Pp = *P. porites*.

prehurricane (Gilbert) level (~18% before summer 1988 vs. ~9% before summer 2005). According to the model, SST anomalies may have lead to marginal bleaching mortalities (absolute losses <5% for each bleaching event).

Predicted rugosity in 2007–2008 (Fig. 4b) was similar to observations and correlated with the predicted total coral cover (Fig. 4c). The observed and predicted coral-rugosity relationships had comparable intercepts (ANCOVA, $P = 0.077$) but slight differences between slopes (ANCOVA, $P = 0.038$). With an hypothetical average rugosity of 1.9 in 1984, the model predicted two acute reductions in architectural complexity related to the 1988 and 2005 hurricane seasons, followed by recovery periods.

The present model fits (Figs 4 and 5) were obtained using a rate of parrotfish erosion of 0.5 kg $CaCO_3$ m^{-2} yr^{-1} and a susceptibility of dead skeletons to hurricanes of 1 (i.e. the probability of breakage of a dead skeleton is the same as its living counterpart). However, other reasonable fits to Cozumel observations were obtained for different combinations of values of bioerosion and breakage susceptibility of dead skeletons, the respective effects of the two erosion parameters being negatively correlated (Appendix S4, Fig. S6). With lower probabilities of breakage for dead skeletons compared to live corals (i.e. breakage susceptibility relative to live corals <1), possible values of bioerosion rates (conditional to an acceptable fit to observations) extended from 0 to 4 kg $CaCO_3$ m^{-2} yr^{-1}. For higher probabilities of breakage (i.e. breakage susceptibility >1), only bioerosion rates below 1 kg $CaCO_3$ m^{-2} yr^{-1} provided an acceptable fit.

Future scenarios of topographical complexity

Model scenarios of future global warming (RCP8.5 business-as-usual GHG emissions) for different hurricane frequencies and local management interventions (Fig. 6) predicted that reef rugosity is likely to respond negatively to future losses of coral cover caused by bleaching. Setting a threshold of rugosity = 1.2 for a nearly flat reef, the model estimated the average time by which different reef topographies may become flat given their present-day amount of corals. Under a scenario of parrotfish management (grazing impact = 40%, bioerosion = 0.5 kg $CaCO_3$ m^{-2} yr^{-1}), low complexity reefs (i.e. present-day reef rugosity between 1.3 and 1.5) may become flat (rugosity <1.2) by 2040 in Caribbean environments subjected to a low hurricane regime (Fig. 6a). The same low complexity reefs, this time in a more severe hurricane environment, may flatten in less than 20 years (i.e. by 2030). Even high complexity reefs (rugosity between 1.8 and 2) may significantly lose structure by 2040. A relatively rich coral cover (i.e. >20%) offers little resistance to a decline of habitat structure driven by global warming, regardless of the hurricane regime. Under a scenario of no management of parrotfish populations (grazing impact = 20%, bioerosion = 0.25 kg $CaCO_3$ m^{-2} yr^{-1}), the deleterious effects of global warming on reef rugosity (Fig. 6b) exceeded those predicted on managed reefs, despite a net reduction in parrotfish erosion associated with reduced grazing.

Discussion

Simulating the dynamics of the reef architectural complexity is challenging because it requires the explicit modelling of mechanisms linking physical processes (those driving the deformation of the reef surface) to biological processes (those controlling the dynamics of the coral reef-builders). Central to a reliable representation of the coral-scale reef topography is the geometry of coral skeletons and their changing surface/volume during the accreting and eroding phases.

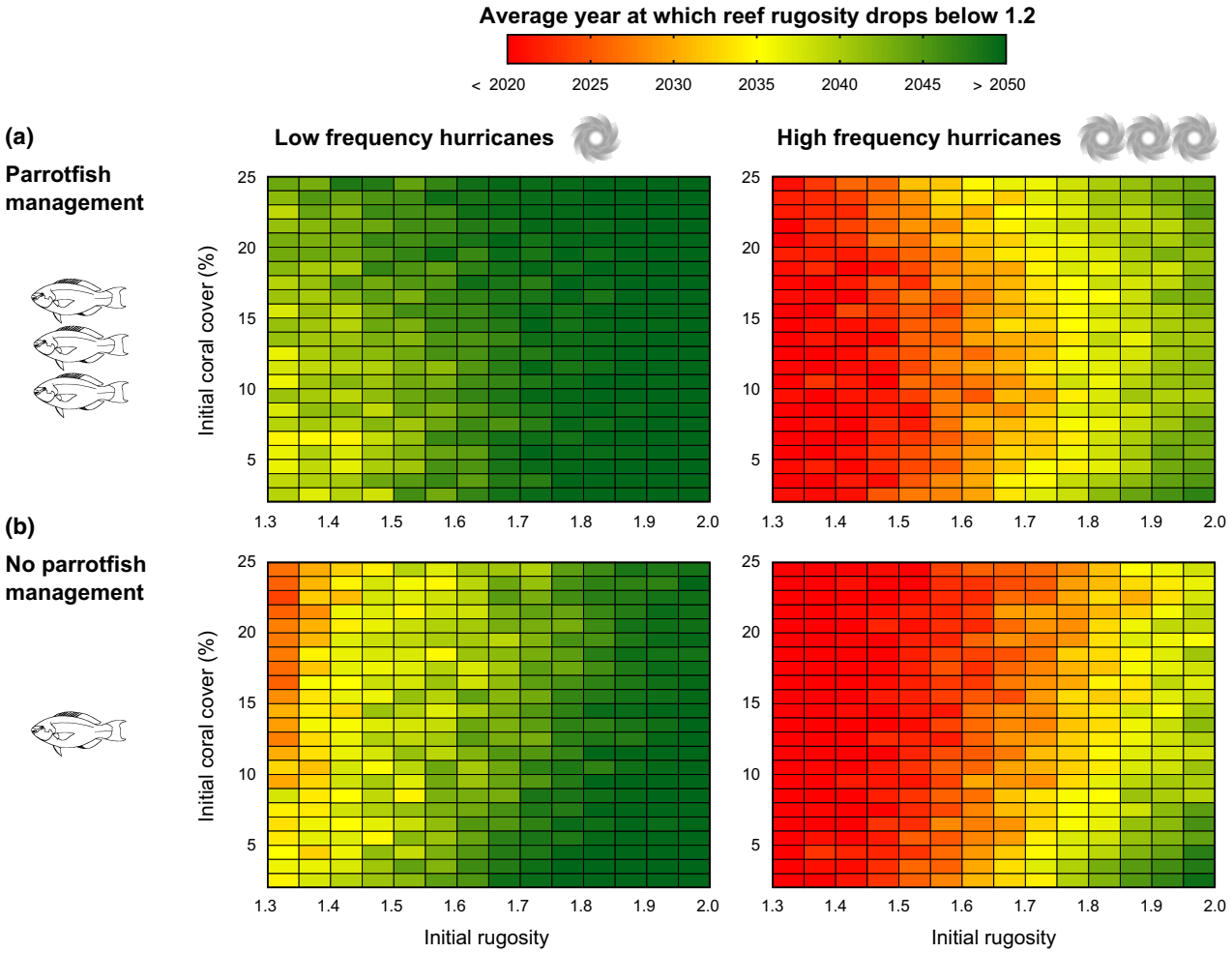

Fig. 6 Future projections (2010–2050) of reef rugosity in the Caribbean under the RCP8.5 global warming scenario, for reefs (a) with and (b) without protection of parrotfish populations from fishing, and low (~every 20 years, left panels) and high (~every 5 years, right panels) frequency of hurricanes. Surface plots display the average year (see key) for a Caribbean reef structure to be critically eroded (rugosity <1.2) given its present-day (2010) coral cover (*y*-axis) and reef rugosity (*x*-axis). Dark green contours indicate a reef rugosity that did not fall below 1.2 by 2050.

Here, using simple morphometrical rules to describe the evolution of massive coral shapes, we developed a mechanistic model of reef rugosity driven by ecological and physical processes. The model simulates the accretion/erosion of the carbonate framework through explicit changes in live/dead coral volumes and actual surface areas, allowing calculation of reef surface roughness similar to the field-based rugosity index. Under reasonable assumptions (i.e. consistent with field observations), the model reproduces the long-term trend of the benthic structure observed on Cozumel reefs. Critically, the model forecasts a general loss of rugosity under climate change scenarios in the Caribbean. Under realistic rates of parrotfish erosion, simulations suggest that protecting parrotfish locally may dampen rather than accelerate the negative impacts of climate-driven disturbances on the reef architecture.

One major assumption of the model is that processes shaping the reef surface are mostly those affecting the surface of live and dead coral skeletons. Hence, coral growth was considered as the primary constructional process of the upper reef framework, ignoring other constructive agents (i.e. encrustation and cementation) that consolidate coral material (Scoffin, 1992; Hubbard *et al.*, 1998; Perry *et al.*, 2008). While it is reasonable to assume that encrustation by secondary framebuilders (e.g. coralline algae and epibiont animals, Scoffin, 1992) do not significantly affect reef topography at the scale it is commonly assessed, simulations did not account for the carbonate sediments and fragments that progressively fill the gaps between coral skeletons. Here, coral

fragments generated by storm were assumed to be transported off the reef whereas it is likely that a significant proportion enter into the constitution of the interlocking framework (Blanchon *et al.*, 1997; Rasser & Riegl, 2002), not only decreasing rugosity but also consolidating the primary carbonate framework thus increasing its resistance to hydrodynamic forces. Moreover, parrotfish grazing is not the only agent of carbonate degradation and many boring organisms significantly erode carbonate skeletons, potentially at similar rates (Tribollet & Golubic, 2011; Perry *et al.*, 2012) but with unknown consequences for the shape of coral skeletons. However, the balanced effects of cementation and internal erosion are accounted for implicitly in the probability of skeletal breakage due to mechanical erosion. The integration of all the constructive and destructive agents of coral reef early diagenesis will require complex and uncertain assumptions, and it is unlikely that an overly complex model based on insufficient knowledge will improve our ability to predict future changes of reef topography. Overall, this model must be regarded as a simplification of the early diagenesis of the upper reef framework, and is obviously not suitable for describing the process of vertical reef accretion over geological times nor for calculating the full carbonate budget of a reef.

Model simulations of coral populations in Cozumel were in close agreement with *in situ* observations, despite discrepancies among survey protocols (Appendix S2). Model and data indicated an overall 50% loss of coral cover on middepth (5–15 m) reefs in southwestern Cozumel in a 25 years time interval. Our study suggests that storms were the main driver of decadal variations of coral cover. Predicted coral bleaching was low, in conformity with the marginal coral mortalities reported along the Mexican coast after the recent mass-bleaching events (McField *et al.*, 2005; Eakin *et al.*, 2010). The presence of very strong currents over the shelf of Cozumel (Muckelbauer, 1990; Alvarez-Filip *et al.*, 2009b) may have protected corals from strong temperature anomalies.

With a disturbance regime dominated by frequent hurricanes (four in 25 years with a minimum category 3), Cozumel reefs appeared to be quite resilient as suggested by the recovery of coral cover (+0.5% per year) between the 1988 and 2005 hurricane damages. The studied period is representative of the hurricane regime recorded in Cozumel over a longer timeframe (one every 7 years on average in the period 1851–2013, Landsea *et al.*, 2014). In addition, resilience to hurricanes is confirmed by the early coral recoveries observed after hurricanes Gilbert (Fenner, 1991) and Emily-Wilma (Alvarez del Castillo-Cardenas *et al.*, 2008). While branching *Acropora* spp. have been uncommon in the recent history of Cozumel (Jordán, 1988; Muckelbauer, 1990; Fenner, 1991), most of the reported loss was due to *A. agaricia* and *P. porites*, two coral species with a delicate skeleton (Fenner, 1991). We expect the recovery could have been higher without the (limited) coral losses caused by hurricane Roxanne (1995) and the successive episodes (1998, 1999) of minor coral bleaching predicted by the model. Other examples of long-term coral recovery in the Western Atlantic are unfortunately uncommon (Roff & Mumby, 2012). Slightly faster recovery rates (+1% per year) have been reported in the US Virgin Islands at St Croix (Bythell *et al.*, 2000) and St John (Edmunds, 2002) for comparable time intervals (7–11 years) and similar reef structures (i.e. moderate to high coral cover dominated by nonbranching corals). In the absence of the fast-growing *Acropora* spp., it is probably unrealistic to expect faster recovery rates on present-day Caribbean coral reefs.

Without historical data on topographical complexity (i.e. earlier than 2007), the variations of reef rugosity predicted by the model are speculative. First, the reconstructed trajectory of rugosity is dependent on the 1984 rugosity average, which is unknown. The most parsimonious assumption was to set initial rugosity to the value (1.90) observed for a similar average coral cover (31%) on the same reefs in 2007–2008, that, like the 1984 sites, lacked *Acropora* (i.e. for *Orbicella*-dominated reefs of similar health). Second, an acceptable fit to observations was provided by different values of mechanical (hurricane-driven) and biological (parrotfish-driven) erosion. The rate of breakage of dead skeletons is difficult to parametrize: whether dead skeletons are more or less susceptible to mechanical stress compared to live coral colonies depends on factors not accounted by the model, such as rates of internal erosion vs. cementation. Higher rates of framework breakage (i.e. breakage susceptibility relative to live corals >1) require rates of parrotfish bioerosion below 0.5 kg $CaCO_3$ m^{-2} yr^{-1}, but such low bioerosion rates would lead to unrealistic high levels of rugosity for reefs that were not damaged by hurricanes. Inversely, lower rates of breakage (relative susceptibility <1) would result in higher bioerosion rates (0.5–4 kg $CaCO_3$ m^{-2} yr^{-1}) with the risk of excessive erosion of reef rugosity. Our choice of a grazing erosion value of 0.5 kg $CaCO_3$ m^{-2} yr^{-1} falls within the upper range of values commonly reported in the Caribbean for similar depths (0.01–0.69 kg $CaCO_3$ m^{-2} yr^{-1}; (Stearn & Scoffin, 1977; Frydl & Stearn, 1978; Bruggemann *et al.*, 1996) although higher values have been recently estimated [1.75–2.17 kg $CaCO_3$ m^{-2} yr^{-1}; (Perry *et al.*, 2012)]. However, starting simulations with a different rugosity value would require different rates of erosion to match the mean rugosity estimated in 2007–2008.

Despite inevitable model limitations, the historical reconstruction of topographical complexity in Cozumel matched the trend observed at the scale of the Caribbean region (Alvarez-Filip *et al*., 2009a). Hence, an initial rugosity of 1.90 is in the range of values reported for *Orbicella*-dominated reefs in the early 1980s. Moreover, the model predicted reef mean rugosity in 1998 to be 1.76, a value very similar to the estimated regional average (1.75) at the same date. After the 1998 mass-bleaching event, Caribbean reef complexity has declined continuously to reach unprecedented low levels (~1.2). Today, Cozumel reefs remain in the upper range of Caribbean reef rugosity, and this may be due to the low incidence of coral bleaching combined with the ability of coral populations to recover from hurricanes. Model simulations thus predicted a recovery of reef rugosity after hurricane Gilbert (Sept. 1988), the regeneration of coral cover being fast enough to offset the erosion of the carbonate framework. This indicates that the carbonate budget of Cozumel reefs may have been positive (i.e. net accreting) during the period 1984–2005, meaning the reef architecture was resilient to severe damages caused by hurricanes.

Our analysis also provides a first approximation of the rate of change in Caribbean reef rugosity in a warming climate, based on coral population dynamics under an intensified bleaching regime and simplified rates of erosion. Although model projections remain uncertain, our findings generate hypotheses about the possible responses of reef topographical complexity to global warming. Under severe and frequent thermal stress caused by business-as-usual GHG emissions, low and medium rugosity (<1.7) reefs may lose structure in the next three decades. Under high frequency hurricane regimes, the same reef habitats may be critically degraded over shorter timescales (<20 years). Coral mortalities due to bleaching disrupted the development of complex architectures and compromised their ability to recover from hurricane damages. It is noteworthy that model forecasts ignored the possible reduction in coral calcification due to chronic warming and acidifying seas. However, some corals may have the ability to acclimate or adapt to elevated temperatures (Palumbi *et al*., 2014), and it is unclear what would be the response of the other organisms involved in the cementation/erosion of the primary carbonate framework. In addition, the effects of ocean warming and acidification are less well recognized for benthic taxa competing with corals and may lead to complex outcomes (Mumby & van Woesik, 2014). While our ability to forecast reef responses to climate change will continually be improved as new data become available, more reliable projections may be achieved by linking the dynamics of the reef topography to a comprehensive carbonate budget. Further developments will also require extending the model to other reef habitats, particularly by depth (e.g. reef flat, shallow forereef and deeper reefs) since the rates of erosion are likely to vary with the habitat preferences of the different eroding organisms.

Under a "business-as-usual" scenario of GHG emissions (RCP 8.5), the ability of Caribbean reefs to maintain functional reef habitats in the short term may depend on the efficiency of local management in sustaining high grazing. As a result, model simulations suggest that with realistic rates of parrotfish bioerosion, high levels of grazing would benefit the reef habitat structure rather than accelerating its degradation (Fig. 6). Protecting or restoring parrotfish grazing may help corals recovering from moderate bleaching and hurricanes (Mumby *et al*., 2014) thus maintaining carbonate production at levels that will offset skeletal erosion (Kennedy *et al*., 2013). Rates of bioerosion of depleted parrotfish stocks, although being much lower than for healthy parrotfish populations, became detrimental to reef rugosity when skeletal production was dramatically reduced. Our results thus support the view of the importance of combining aggressive mitigation of GHG emissions with local interventions aiming at favouring a net coral growth.

Forecasting the quality of the reef architecture is crucial to envision the future provision of reef habitats. By simulating an explicit reef habitat structure, the present model offers new perspectives for the projection of coral reef futures under warming scenarios. For instance, it may be possible to forecast the responses of ecosystem function and services to gradual changes in the reef architecture, providing simple relationships between topographical complexity and the diversity, density or biomass of the associated motile fauna (Graham *et al*., 2006; Wilson *et al*., 2010; Graham & Nash, 2013; Nash *et al*., 2013; Rogers *et al*., 2014). Here, reef architectural complexity was modelled by simulating the extension/reduction in the reef bottom, the net outcome being quantified by a simple ratio between the reef surface area and its horizontal projection. Such a ratio gives little indication about the actual shape of the reef surface which determines the *quality* of the habitat structure (e.g. the relative proportion of convex vs. concave surfaces, the size of holes and crevices or the presence of overhangs). However, the same limitation affects field-based rugosity measurements: the "chain-and-tape" method is not able to discriminate the shape and size of the structural elements of the reef substrate (McCormick, 1994; Shumway *et al*., 2007) because different textures (or profiles) can produce similar surfaces (or contours). While model developments are required to improve the simulation of the reef architecture (e.g. by integrating the growth and erosion of complex coral

shapes), further empirical data are needed to support model parametrization and calibration. This includes a better quantification of topographical complexity and the production of time-series through repeated sampling of the reef architecture. In this regard, fine-scale bathymetric reconstructions created from underwater imagery (e.g. Friedman *et al.*, 2012) appear as a promising support for model development. Such methods may also improve reef monitoring, because a gradual loss of habitat structure may go unnoticed until detrimental effects on reef-associated organisms become evident. Clearly, more precise data and models will benefit the monitoring and the management of reef-associated services by focusing intervention on the maintenance of functional reef habitats.

Acknowledgements

The research leading to these results has received funding from the European Union 7th Framework programme (P7/2007-2013) under grant agreement No. 244161 (FORCE project), a NERC grant and ARC Laureate Fellowship to PJM. We thank D. Fenner, E. Jordán-Dahlgren and G. Muckelbauer for providing information related to early surveys on Cozumel reefs. Coral morphometric data were collected with the permission and support of the Parque Nacional Arrecifes de Cozumel and the Comisión Nacional de Áreas Naturales Protegidas of México. We also thank I. Chollett for formatting the historical SST time-series of Cozumel, P. Halloran for providing the SST forecasts for the climate change scenarios, and G. Roff and J.C. Ortiz for fruitful discussions.

References

Alvarez del Castillo-Cardenas PA, Reyes-Bonilla H, Alvarez-Filip L, Millet-Encalada M, Escobosa-Gonzalez LE (2008) *Cozumel Island, Mexico: a disturbance history*. Proceedings of the 11th International Coral Reef Symposium, 701–705. Ft. Lauderdale, Florida.

Alvarez-Filip L, Dulvy NK, Gill JA, Côté IM, Watkinson AR (2009a) Flattening of Caribbean coral reefs: region-wide declines in architectural complexity. *Proceedings of the Royal Society B: Biological Sciences*, **276**, 3019–3025.

Alvarez-Filip L, Millet-Encalada M, Reyes-Bonilla H (2009b) Impact of Hurricanes Emily and Wilma on the coral community of Cozumel Island, Mexico. *Bulletin of Marine Science*, **84**, 295–306.

Alvarez-Filip L, Dulvy NK, Côté IM, Watkinson AR, Gill JA (2011) Coral identity underpins architectural complexity on Caribbean reefs. *Ecological Applications*, **21**, 2223–2231.

Anthony K, Maynard JA, Diaz-Pulido G, Mumby PJ, Marshall PA, Cao L, Hoegh-Guldberg O (2011) Ocean acidification and warming will lower coral reef resilience. *Global Change Biology*, **17**, 1798–1808.

Bellwood DR, Choat JH (1990) A functional analysis of grazing in parrotfishes (family Scaridae): the ecological implications. *Environmental Biology of Fishes*, **28**, 189–214.

Blanchon P, Jones B, Kalbfleisch W (1997) Anatomy of a fringing reef around Grand Cayman: storm rubble, not coral framework. *Journal of Sedimentary Research*, **67**, 1–16.

Bruggemann JH, Van Kessel AM, Van Rooij JM, Breeman AM (1996) Bioerosion and sediment ingestion by the Caribbean parrotfish *Scarus vetula* and *Sparisoma viride*: implications of fish size, feeding mode and habitat use. *Marine Ecology Progress Series*, **134**, 59–71.

Bruno JF, Selig ER (2007) Regional decline of coral cover in the Indo-Pacific: timing, extent, and subregional comparisons. *PLoS ONE*, **2**, e711.

Bythell JC, Hillis-Starr ZM, Rogers CS (2000) Local variability but landscape stability in coral reef communities following repeated hurricane impacts. *Marine Ecology Progress Series*, **204**, 93–100.

De'ath G, Lough JM, Fabricius KE (2009) Declining coral calcification on the Great Barrier Reef. *Science*, **323**, 116–119.

Done TT, Ogden JJ, Wiebe W, Rosen B (1996) Biodiversity and ecosystem function of coral reefs. In: *Functional Roles of Biodiversity: A Global Perspective* (eds Mooney HA, Cushman JH, Medina E, Sala OE, Schulze E-D), pp. 393–429. John Wiley and Sons, Chichester.

Eakin CM, Morgan JA, Heron SF *et al.* (2010) Caribbean corals in crisis: record thermal stress, bleaching, and mortality in 2005. *PLoS ONE*, **5**, e13969.

Edmunds PJ (2002) Long-term dynamics of coral reefs in St. John, US Virgin Islands. *Coral Reefs*, **21**, 357–367.

Edwards HJ, Elliott IA, Eakin CM *et al.* (2011) How much time can herbivore protection buy for coral reefs under realistic regimes of hurricanes and coral bleaching? *Global Change Biology*, **17**, 2033–2048.

Fenner DP (1988) Some leeward reefs and corals of Cozumel, Mexico. *Bulletin of Marine Science*, **42**, 133–144.

Fenner DP (1991) Effects of Hurricane Gilbert on coral reefs, fishes and sponges at Cozumel, Mexico. *Bulletin of Marine Science*, **48**, 719–730.

Friedman A, Pizarro O, Williams SB, Johnson-Roberson M (2012) Multi-scale measures of rugosity, slope and aspect from benthic stereo image reconstructions. *PLoS ONE*, **7**, e50440.

Frieler K, Meinshausen M, Golly A, Mengel M, Lebek K, Donner SD, Hoegh-Guldberg O (2012) Limiting global warming to 2°C is unlikely to save most coral reefs. *Nature Climate Change*, **3**, 165–170.

Frydl P, Stearn CW (1978) Rate of bioerosion by parrotfish in Barbados reef environments. *Journal of Sedimentary Research*, **48**, 1149–1158.

Gardner TA, Côté IM, Gill JA, Grant A, Watkinson AR (2003) Long-term region-wide declines in Caribbean corals. *Science*, **301**, 958–960.

Glynn PW (1997) Bioerosion and coral-reef growth: a dynamic balance. In: *Life and Death of Coral Reefs* (ed. Birkeland C), pp. 68–95. Chapman and Hall, New York.

Graham NAJ, Nash KL (2013) The importance of structural complexity in coral reef ecosystems. *Coral Reefs*, **32**, 315–326.

Graham NA, Wilson SK, Jennings S, Polunin NV, Bijoux JP, Robinson J (2006) Dynamic fragility of oceanic coral reef ecosystems. *Proceedings of the National Academy of Sciences*, **103**, 8425–8429.

Hixon MA, Beets JP (1993) Predation, prey refuges, and the structure of coral-reef fish assemblages. *Ecological Monographs*, **63**, 77–101.

Hoegh-Guldberg O, Mumby PJ, Hooten AJ *et al.* (2007) Coral reefs under rapid climate change and ocean acidification. *Science*, **318**, 1737–1742.

Hubbard DK, Burke RB, Gill IP (1998) Where's the reef: the role of framework in the Holocene. *Carbonates and Evaporites*, **13**, 3–9.

Hutchings PA (1986) Biological destruction of coral reefs. *Coral Reefs*, **4**, 239–252.

Johns TC, Durman CF, Banks HT *et al.* (2006) The new Hadley Centre climate model (HadGEM1): evaluation of coupled simulations. *Journal of Climate*, **19**, 1327–1353.

Jones GP (1991) Postrecruitment processes in the ecology of coral reef fish populations: a multifactorial perspective. In:*The Ecology of Fishes on Coral Reefs* (ed. Sale PF), pp. 294–328. Academic Press, New York.

Jones GP, Syms C (1998) Disturbance, habitat structure and the ecology of fishes on coral reefs. *Australian Journal of Ecology*, **23**, 287–297.

Jordán E (1988) Arrecifes profundos en la Isla de Cozumel, México. *Anales del Instituto de Ciencias del Mar y Limnologia, UNAM*, **15**, 195–208.

Kennedy EV, Perry CT, Halloran PR *et al.* (2013) Avoiding coral reef functional collapse requires local and global action. *Current Biology*, **23**, 912–918.

Knudby A, LeDrew E (2007) Measuring structural complexity on coral reefs. In: *Diving for Science 2007*. Proceedings of the American Academy of Underwater Sciences 26th Symposium (eds Pollock N, Godfrey J), pp. 181–188. Miami, Florida.

Landsea C, Franklin J, Beven J (2014) The revised Atlantic hurricane database (HURDAT2). Available at: http://www.aoml.noaa.gov/hrd/hurdat/Data_Storm.html (accessed 16 July 2014).

Luckhurst BE, Luckhurst K (1978) Analysis of the influence of substrate variables on coral reef fish communities. *Marine Biology*, **49**, 317–323.

Mallela J, Perry CT (2007) Calcium carbonate budgets for two coral reefs affected by different terrestrial runoff regimes, Rio Bueno, Jamaica. *Coral Reefs*, **26**, 129–145.

McCormick MI (1994) Comparison of field methods for measuring surface topography and their associations with a tropical reef fish assemblage. *Marine Ecology Progress Series*, **112**, 87–96.

McField M, Bood N, Fonseca A, Arrivillaga A, Franquesa Rinos A, Loreto Viruel R (2005) Status of the Mesoamerican Reef after the 2005 coral bleaching event. In: *Status of Caribbean coral reefs after bleaching and hurricanes in 2005* (eds Wilkinson C, Souter D), pp. 45–60. Global Coral Reef Monitoring Network, and Reef and Rainforest Research Centre, Townsville.

Muckelbauer G (1990) The shelf of Cozumel, Mexico: topography and organisms. *Facies*, **23**, 201–239.

Mumby PJ (2006) The impact of exploiting grazers (Scaridae) on the dynamics of Caribbean coral reefs. *Ecological Applications*, **16**, 747–769.

Mumby PJ, van Woesik R (2014) Consequences of ecological, evolutionary and biogeochemical uncertainty for coral reef responses to climatic dtress. *Current Biology*, **24**, R413–R423.

Mumby PJ, Hedley JD, Zychaluk K, Harborne AR, Blackwell PG (2006) Revisiting the catastrophic die-off of the urchin Diadema antillarum on Caribbean coral reefs: fresh insights on resilience from a simulation model. *Ecological Modelling*, **196**, 131–148.

Mumby PJ, Hastings A, Edwards HJ (2007) Thresholds and the resilience of Caribbean coral reefs. *Nature*, **450**, 98–101.

Mumby PJ, Steneck RS, Hastings A (2013) Evidence for and against the existence of alternate attractors on coral reefs. *Oikos*, **122**, 481–491.

Mumby PJ, Wolff NH, Bozec Y-M, Chollett I, Halloran P (2014) Operationalizing the resilience of coral reefs in an era of climate change. *Conservation Letters*, **7**, 176–187.

Nash KL, Graham NA, Wilson SK, Bellwood DR (2013) Cross-scale habitat structure drives fish body size distributions on coral reefs. *Ecosystems*, **16**, 478–490.

Ong L, Holland KN (2010) Bioerosion of coral reefs by two Hawaiian parrotfishes: species, size differences and fishery implications. *Marine Biology*, **157**, 1313–1323.

Palumbi SR, Barshis DJ, Traylor-Knowles N, Bay RA (2014) Mechanisms of reef coral resistance to future climate change. *Science*, **344**, 895–898.

Perry CT, Spencer T, Kench PS (2008) Carbonate budgets and reef production states: a geomorphic perspective on the ecological phase-shift concept. *Coral Reefs*, **27**, 853–866.

Perry CT, Edinger EN, Kench PS, Murphy GN, Smithers SG, Steneck RS, Mumby PJ (2012) Estimating rates of biologically driven coral reef framework production and erosion: a new census-based carbonate budget methodology and applications to the reefs of Bonaire. *Coral Reefs*, **31**, 853–868.

Perry CT, Murphy GN, Kench PS, Smithers SG, Edinger EN, Steneck RS, Mumby PJ (2013) Caribbean-wide decline in carbonate production threatens coral reef growth. *Nature Communications*, **4**, 1402.

Pratchett MS, Hoey AS, Wilson SK (2014) Reef degradation and the loss of critical ecosystem goods and services provided by coral reef fishes. *Current Opinion in Environmental Sustainability*, **7**, 37–43.

Rasser M, Riegl B (2002) Holocene coral reef rubble and its binding agents. *Coral Reefs*, **21**, 57–72.

Riahi K, Rao S, Krey V *et al*. (2011) RCP 8.5 - A scenario of comparatively high greenhouse gas emissions. *Climatic Change*, **109**, 33–57.

Risk MJ (1972) Fish diversity on a coral reef in the Virgin Islands. *Atoll Research Bulletin*, **153**, 1–6.

Roff G, Mumby PJ (2012) Global disparity in the resilience of coral reefs. *Trends in Ecology & Evolution*, **27**, 404–413.

Rogers CS, Suchanek TH, Pecora FA (1982) Effects of hurricanes David and Frederic (1979) on shallow *Acropora palmata* reef communities: St. Croix, US Virgin Islands. *Bulletin of Marine Science*, **32**, 532–548.

Rogers A, Blanchard JL, Mumby PJ (2014) Vulnerability of coral reef fisheries to a loss of structural complexity. *Current Biology*, **24**, 1000–1005.

Scoffin TP (1992) Taphonomy of coral reefs: a review. *Coral Reefs*, **11**, 57–77.

Shinn EA, Hudson JH, Halley RB, Lidz B, Robbin DM, Macintyre IG (1982) Geology and sediment accumulation rates at Carrie Bow Cay, Belize. *Smithsonian Contributions to the Marine Sciences*, **12**, 63–75.

Shumway CA, Hofmann HA, Dobberfuhl AP (2007) Quantifying habitat complexity in aquatic ecosystems. *Freshwater Biology*, **52**, 1065–1076.

Stearn CW, Scoffin TP (1977) *Carbonate budget of a fringing reef, Barbados*. Proceedings of the 3rd International Coral Reef Symposium, 2, 471–476. Miami, FL.

Stearn CW, Scoffin TP, Martindale W (1977) Calcium carbonate budget of a fringing reef on the west coast of Barbados. Part I. Zonation and productivity. *Bulletin of Marine Science*, **27**, 479–510.

Steneck RS (1994) Is herbivore loss more damaging to reefs than hurricanes? Case studies from two Caribbean reef systems (1978–1988). Proceedings of the Colloquium on Global Aspects of Coral Reefs: Health, Hazards and History (ed. Ginsburg RN), pp. 220–226. Miami, FL.

Stine WB, Geyer N (2001) Power from the Sun. Available at: http://www.powerfromthesun.net/index.htm (accessed 5 May 2014).

Syms C, Jones GP (2000) Disturbance, habitat structure, and the dynamics of a coral-reef fish community. *Ecology*, **81**, 2714–2729.

Tribollet A, Golubic S (2011) Reef bioerosion: agents and processes. In: *Coral Reefs: An Ecosystem in Transition* (eds Dubinsky Z, Stambler N), pp. 435–449. Springer, Berlin.

Wilson SK, Fisher R, Pratchett MS *et al*. (2010) Habitat degradation and fishing effects on the size structure of coral reef fish communities. *Ecological Applications*, **20**, 442–451.

Woodley JD, Chornesky EA, Cliffo PA *et al*. (1981) Hurricane Allen's impact on Jamaican coral reefs. *Science*, **214**, 13.

Supporting Information

Additional Supporting Information may be found in the online version of this article:

Appendix S1. Model description and parametrization.
Appendix S2. Cozumel coral reef data 1984–2008.
Appendix S3. Additional results of the analysis of coral morphometrics.
Appendix S4. Model fits to Cozumel data for different erosion values.